Anal. Chem. **2004,** *76,* 2112−2117

Denaturation and Renaturation of Self-Assembled Yeast Iso-1-cytochrome *c* on Au

Soonwoo Chah,[†] Challa V. Kumar,[‡] Matthew R. Hammond,[†] and Richard N. Zare*,[†]

Department of Chemistry, Stanford University, Stanford, California 94305, and Department of Chemistry, University of Connecticut, Storrs, Connecticut 06269-4060

We have made surface plasmon resonance (SPR) measurements of yeast iso-1-cytochrome *c* (Cyt *c*) on a gold surface. Angle-resolved SPR curves are recorded as a function of urea concentration before and after self-assembly of the Cyt *c*. Exposure to a urea solution causes denaturation of Cyt *c*, which shifts the minimum in the SPR curve to a larger angle and decreases the signal amplitude. The Gibbs free energy change for denaturation of the protein on Au is calculated from the change of the SPR signal amplitude with urea concentration. We find that (1) Cyt *c* can be reversibly denatured and renatured, depending on the urea concentration, and (2) the Gibbs free energy change for denaturation of Cyt *c* on Au surface in water, ΔG°_{water}, is 1.5 kcal/mol, which is ∼4 times less than that in bulk solution.

Researchers have been exploiting the properties of biomolecules for specific practical functions, with high selectivity and sensitivity, as biosensors or as efficient catalysts.[1,2] When they are used in a practical way, they are usually immobilized on solid supports for purposes such as separation and reuse.[3,4] However, immobilization of biomolecules on solid supports often results in reduced activity when compared to the activities in bulk solution. Conformational changes or other effects arising from the interaction between the biomolecule and the support can cause the loss of activity.[5]

For this reason, quantification of bioactivities of molecules attached to a solid surface is important not only in fundamental chemistry aspects but also in designing biosensors or biocatalysts. The bioactivity is related to the stability as well as conformation of biomolecules, and the stability can be determined by measuring thermodynamics properties. An example is the Gibbs free energy change ΔG° for denaturation. Even though thermodynamic properties of biomolecules in bulk phase have been studied for a long time,[6] determining the Gibbs free energy change for denaturation at solid supports is a challenging task.

The surface plasmon resonance (SPR) technique has been widely used to investigate antigen−antibody interactions or to obtain their kinetics and equilibrium constants.[7−9] SPR is also being used for various applications from chemical and biological sensors to hybridization of DNAs or to immunological assays that have been combined with microfluidics.[10−15] SPR is a phenomenon that occurs when linearly polarized light whose electric vector is perpendicular to the surface (p-polarized) propagates from a high-refractive-index material toward an interface with a low-refractive-index material. When the incoming light strikes the surface at an incident angle larger than the critical angle, an evanescent wave is created that penetrates a short distance into the lower-index medium. When a thin metal (usually gold or silver) layer is placed at this interface, the evanescent wave couples to the electrons in the metal, thereby reducing the intensity of the reflected light (R/R_0). The minimum reflectivity occurs at a particular incident angle called the SPR angle, θ_{SPR}.[16−18] The position of θ_{SPR}, the width of the SPR plot, and the reflectivity ($(R/R_0)_{min}$) at θ_{SPR} for which R/R_0 is a minimum are highly sensitive to the dielectric constant and the thickness of the material in contact with the metal surface.[19]

Proteins in their native state are structurally compact whereas those in the denatured state are comparatively loose, take up a random coil conformation, and show less biological activity. The conformational changes induced by denaturation or renaturation

* Corresponding author. E-mail: zare@stanford.edu.
[†] Stanford University.
[‡] University of Connecticut.

(1) Stocker, J.; Balluch, D.; Gsell, M.; Harms, H.; Feliciano, J.; Daunert, S.; Malik, K. A.; van der Meer, J. R. *Environ. Sci. Technol.* **2003**, *37* (20), 4743−4750.
(2) Nakamura, F.; Ito, E.; Sakao, Y.; Ueno, N.; Gatuna, I. N.; Ohuchi, F. S.; Hara, M. *Nano Lett.* **2003**, *3*, 1083−1086.
(3) Besteman, K.; Lee, J.-O.; Wiertz, F. G. M.; Heering, H. A.; Dekker: C. *Nano Lett.* **2003**, *3*, 727−730.
(4) Betancor, L.; Hidalgo, A.; Fernandez-Lorente, G.; Mateo, C.; Fernandez-Lafuente, R.; Guisan, J. M. *Biotechnol. Prog.* **2003**, *19*, 763−767.
(5) Neumann, L.; Wohland, T.; Whelan, R. J.; Zare, R. N.; Kobilka, B. K. *ChemBioChem* **2002**, *3*, 993−998.
(6) Gupta, R.; Ahmad, F. *Biochemistry* **1999**, *38*, 2471−2479.
(7) Georgiadis, R.; Peterlinz, K. P.; Peterson, A. W. *J. Am. Chem. Soc.* **2000**, *122*, 3166−3173.
(8) Sota, H.; Hasegawa, Y.; Iwakura, M. *Anal. Chem.* **1998**, *70*, 2019−2024.
(9) Schubert, F.; Zettl, H.; Häfner, W.; Krauss, G.; Krausch, G. *Biochemistry* **2003**, *42* (34), 10288−10294.
(10) Arakawa T. Miwa, S. *Thin Solid Films* **1996**, *281−282*, 466−468.
(11) Jaffrezic-Renault, N.; Abdelghani, A.; Chovelon, J. M.; Ronot-Trioli, C.; Veillas, C.; Gagnaire, H. *Sens. Actuators, B* **1997**, *39*, 407−410.
(12) Koh, S. S.; Ansari, A. Z.; Ptashne, M.; Young, R. A. *Mol. Cell* **1998**, *1*, 895−904.
(13) Wegner, G. J.; Lee, H. J.; Corn, R. M. *Anal. Chem.* **2002**, *74*, 5161−5168.
(14) Wheeler, A. R.; Chah, S.; Whelan, R. J.; Zare, R. N. *Sens. Actuators, B*, in press.
(15) Wegner, G. J.; Lee, H. J.; Marriott, G.; Corn, R. M. *Anal. Chem.* **2003**, *75*, 4740−4746.
(16) Jordan C. E.; Corn, R. M. *Anal. Chem.* **1997**, *69*, 1449−1456.
(17) Lyon, L. A.; Peña, D. J.; Natan, M. J. *J. Phys. Chem. B* **1999**, *103*, 5826−5831.
(18) He, L.; Musick, M. D.; Nicewarner, S. R.; Salinas, F. G.; Benkovic, S. J.; Natan, M. J. *J. Am. Chem. Soc.* **2000**, *122*, 9071−9077.
(19) Hutter, E.; Cha, S.; Liu, J.-F.; Park, J.; Yi, J.; Fendler, J. H.; Roy, D. *J. Phys. Chem. B* **2001**, *105*, 8−12.

10.1021/ac035416k CCC: $27.50
Published on Web 03/09/2004

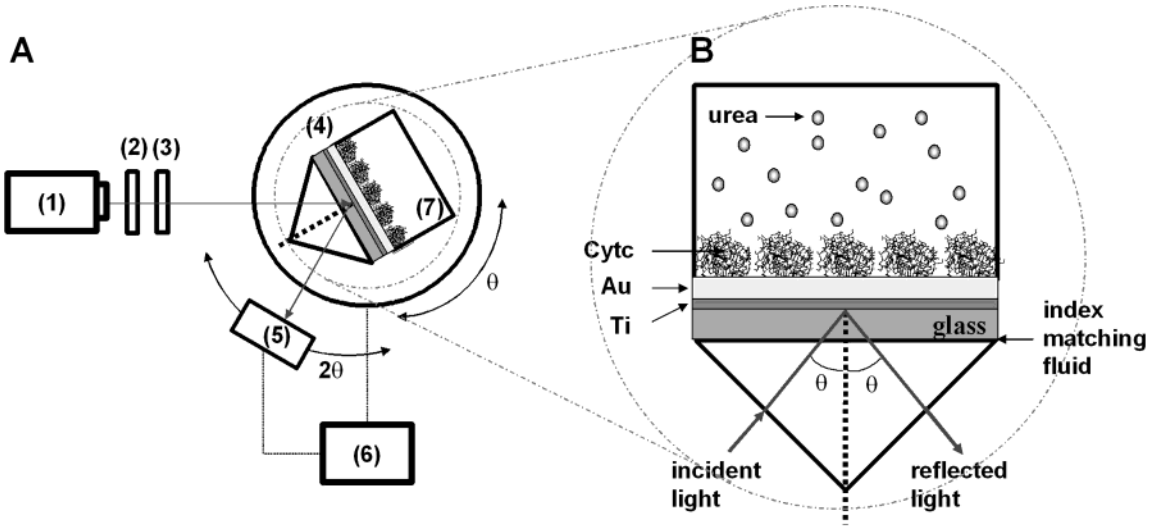

Figure 1. (A) Schematic diagram of a surface plasmon resonance setup. Incoming light is reflected to a detector by the gold film, which is evaporated on SF10 glass, following the deposition of a binding layer of Ti. When the rotation stage turns by an angle θ, the detector moves 2θ: (1) laser, (2) polarizer, (3) convex lens, (4) rotation stage, (5) detector, (6) computer, and (7) Teflon cell. (B) Enlargement of a reaction cell. For the formation of Cyt *c* self-assembled layer on Au, the solution in Teflon cell is replaced with Cyt *c* solution. After self-assembly, the effect of urea solution on denaturation of Cyt *c* is examined by substituting the solution in a cell with a solution at a given urea concentration.

of biomolecules on a solid affect the dielectric constant and the thickness of the layer adjacent to the Au film; they are expressed by changes in the SPR plot, such as shifts of θ_{SPR} and $(R/R_0)_{min}$ or changes in width. Therefore, monitoring these parameters enables us to investigate the denaturation or renaturation of biomolecules. Furthermore, it facilitates the calculation of the Gibbs free energy change of biomolecules bound to solid surfaces. Here, we demonstrate a methodology to quantify denaturation of biomolecules at a solid−liquid interface in the presence of a denaturant using SPR.

As a first demonstration of this technique, we have investigated the denaturation of cytochrome *c* (Cyt *c*) from the unicellular yeast species *Saccharomyces cerevisiae*. Cyt *c* is a heme protein, and it is central to the chain of electron-transfer reactions that participate in mitochondrial respiration. Cyt *c*, in addition, has a single Cys residue near the surface and this feature can be utilized to form a self-assembled monolayer (SAM) of Cyt *c* at Au. Furthermore, Cyt *c* is known to undergo reversible denaturation, and its behavior at several solid surfaces has been investigated. We self-assembled Cyt *c* on Au and compared SPR plots for bare Au with those for biomolecule-adsorbed Au as a function of urea concentration. The difference in the two sets of SPR curves enables us to calculate the Gibbs free energy change of Cyt *c* at the solid−liquid interface when it interacts with urea, which causes this biomolecule to alter its conformation, that is, to denature.

EXPERIMENTAL SECTION

Materials. Cyt *c* from *S. cerevisiae* (yeast iso-1-cytochrome *c*; Aldrich) and 3-mercaptopropionic acid (MPA, Aldrich) were used as received. Urea (J. T.Baker Inc.), a denaturant, was dissolved in 10 mM potassium phosphate buffer (Mallinckrodt, pH 7.2) to prepare urea solutions of different concentrations up to 7 M. Sulfuric acid (Fisher Scientific) and hydrogen peroxide (Fisher Scientific) were used to clean the microscope slide glasses on which titanium and gold films were deposited. H_2O was purified to more than 18 MΩ using a Milli-Q water system (Millipore).

Preparation of Gold Substrates. Microscope slides (3 in. × 1 in. SF10 glass, Schott Glass Technology) were immersed in a piranha solution (sulfuric acid:hydrogen peroxide = 70:30 vol %) for 2 min prior to the metal evaporation (Caution: this solution is extremely toxic and corrosive and should be handled appropriately with great care.). The slides were rinsed with water several times and dried with nitrogen. Then, Au films were deposited on the clean SF10 slides in a home-built vacuum chamber using Ti binder layers. Ti was deposited to obtain a good adhesion between Au and SF10 glass. A quartz crystal microbalance (QCM) was used to monitor the weight of the Ti and Au films, which were 2 and 44 nm in thickness, respectively. The gold substrates were cut into small pieces (1 cm × 1 cm) and kept in the dark until they were used.

SPR System. The time-resolved and angle-resolved SPR measurements were carried out for the analyses of self-assembled layers using a home-built SPR setup. Figure 1 presents a schematic diagram of the SPR instrument used in this work. A cleaned gold substrate was attached to a SF10 prism (1.5 cm × 1.5 cm right-angle prism, CVI) with index matching fluid ($n = 1.730 \pm 0.0005$, R. P. Cargille Laboratories, Inc.). A Teflon cell was attached to the gold substrate to hold the solution. The 658-nm output of a 30-mW diode laser (LDCU5/4953, Power Technologies) was p-polarized and focused by a lens through the prism onto the gold substrate. The cell had an O-ring (i.d. = 0.6 cm). Laser light contacted the solution in the middle of the O-ring. Both the prism and the cell were mounted on a rotating plate to control the angle of the incident light. The light reflected from the gold substrate was viewed by a split-field photodiode detector (S2721-02, Hamamatsu) and a power meter (PD200, OPHIR) for time-resolved and angle-resolved measurements, respectively. Data were collected by a computer connected to the experimental apparatus.

Modification of Gold Substrates. First, we measured angle-resolved SPR curves on a bare gold substrate as a function of

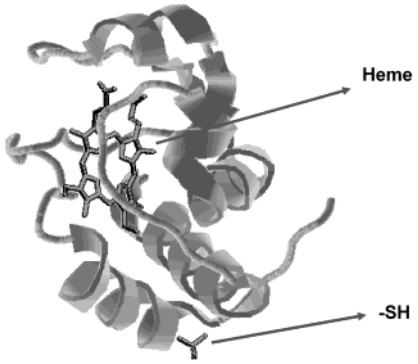

Figure 2. Crystal structure of cytochrome *c* from unicellular yeast species *S. cerevisiae* (yeast iso-1-cyrochrome *c*).[21,22] The molecule has an iron protoprophyrin ix (heme) and a thiol group from a single free cysteine amino acid that facilitates its self-assembly on a Au surface.

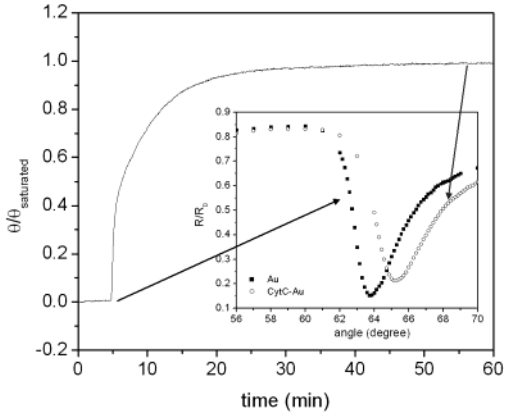

Figure 3. Normalized time-resolved SPR signal of Cyt *c*. The gold surface became covered with Cyt *c* in 1 h. Inset shows the angle-resolved SPR curves for a bare Au and Cyt *c*-saturated Au, respectively. During the self-assembly of Cyt *c*, the SPR angle changed from 64.79° to 65.29°.

urea concentration. The concentration of urea was varied from 0 to 6 M in steps of 0.5 M. After these measurements, the prism in contact with the gold substrate was rotated to the SPR angle and the cell was loaded with 10 mM potassium phosphate buffer solution (0 M urea solution). While the reflectance was monitored, the solution in a cell was replaced with 35 μM Cyt *c* dissolved in the buffer. The change of SPR signal was initiated by the contact of Cyt *c* on gold and continued until Cyt *c*-SAM formation was complete. Time-resolved data at the SPR angle were collected every 3 s for 4 h. After saturation of the SPR signal from adsorption of Cyt *c* on Au occurred, the cell was washed with water and buffer several times and filled with the buffer solution. The washes removed nonspecifically bound Cyt *c*. A set of angle-resolved SPR curves was collected with the Cyt *c*-adsorbed Au substrate as a function of urea concentration. It is well known that urea fully denatures Cyt *c* at ~7 M in bulk solution.[6,20] The difference between the two sets of angle-resolved SPR results was analyzed to extract the denaturation effect of urea on Cyt *c*. For comparison, all the procedures were repeated using MPA as the adsorbate instead of Cyt *c*. We chose MPA because it is not denatured by urea.

RESULTS AND DISCUSSION

Self-Assembly of Cyt *c* on Gold. Cytochrome *c* has a typical protein structure where the heme is surrounded by apoprotein,[21,22] as shown in Figure 2. Yeast iso-1-cytochrome *c* (Cyt *c*) especially has a free thiol group, which allows it to form a firm self-assembled monolayer on a gold surface. In addition, the values of its thermodynamic properties in bulk phase have been published.[23] This fact enables us to compare the data with the data obtained when Cyt *c* is attached to the gold surface.

Prior to the investigation of the denaturation effect of urea on Cyt *c*, we needed to monitor the formation of Cyt *c* monolayer on the gold surface. Figure 3 shows time-resolved and angle-resolved SPR curves of the Cyt *c*-SAM we prepared. The Cyt *c* began to be adsorbed immediately after the gold surface made contact with the protein solution (35 μM Cyt *c*, 10 mM phosphate buffer). It formed a saturated film in 1 h, which moved angle-resolved SPR data by 0.5° to the right and 0.061 upward (in R/R_0). Further washings did not remove the protein, which indicates firm attachment of the protein to the solid. The adsorption of Cyt *c* on the Au surface was also supported by X-ray photoelectron spectroscopy (XPS, S-Probe Monochromatized XPS spectrometer employing Al(Kα) radiation (1486 eV) as a probe, Surface Science Instruments). The XPS data indicated that the surface was composed of 18.60% O (1s), 15.38% N (1s), 59.18% C (1s), and 6.85% Au (4f).

Denaturation of Cyt *c* on Gold Surface by Urea. One of the characteristics of SPR is that it is sensitive to changes in the spatial layer of ~200-nm thickness that covers the metal layer. These changes may result from the presence of a nonbinding high-refractive-index solution or the immobilization of molecules to the gold substrate.[24] Before and after the self-assembly of Cyt *c* on Au, angle-resolved SPR curves at several urea concentrations (0−6 M) were obtained. Figure 4 shows a comparison of the resulting measurements. The SPR plots for bare Au (Figure 4a) proportionally shifted right depending on urea concentration without changes in reflectivity at the resonant angles $(R_{Au}/R_0)_{min}$ for different urea conditions. On the contrary, the SPR curves measured with Cyt *c*−Au (Figure 4b) showed not only a shift to the right but also a decrease in the reflectivity at the resonant angle $(R_{Cyt\ c}/R_0)_{min}$ up to a concentration of 5 M urea, followed by no further changes above 5 M urea.

In general, the complex refractive index N of a solution can be expressed in the form of $N = n + ik$, where the real part n is the index of refraction, and the imaginary part k is the extinction coefficient. The real ϵ' and imaginary ϵ'' parts of the dielectric constant are related to N by the equations $\epsilon' = n^2 - k^2$ and $\epsilon'' = 2nk$.[25] The imaginary part of the dielectric constant of urea is zero

(20) Gianni, S.; Brunori, M.; Travaglini-Allocatelli, C. *Protein Sci.* **2001**, *10*, 1685−1688.
(21) Wood, L. L.; Cheng, S.; Edmiston, P. L.; Saavedra, S. S. *J. Am. Chem. Soc.* **1997**, *119*, 571−576.
(22) Louie, G. V.; Brayer, G. D. *J. Mol. Biol.* **1990**, *214*, 527−555. The protein structure of Cyt *c* (PDB ID: 1YCC) was obtained from the protein data bank (PDB) website (http://www.rcsb.org/pdb/).
(23) Huyghues-Despointes, B. M. P.; Scholtz, J. M.; Pace, C. N. *Nat. Struct. Biol.* **1999**, *6*, 910−912.
(24) Whelan, R. J.; Zare, R. N. *Anal. Chem.* **2003**, *75*, 1542−1547.
(25) *CRC Handbook of Chemistry and Physics*, 83rd ed.; CRC Press Inc.: Boca Raton, FL, 2002.

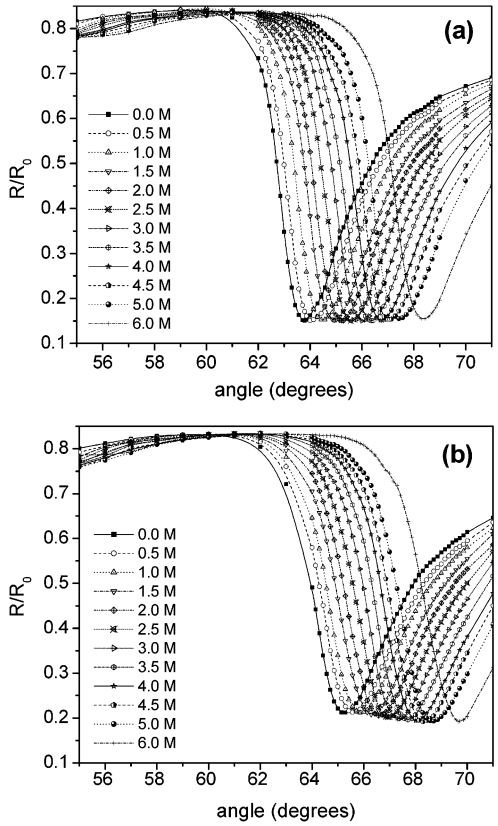

Figure 4. Angle-resolved SPR curves as a function of urea concentration (a) for bare Au and (b) for Cyt *c*−Au. Both curves shift right at high concentrations of urea. Reflectivity at resonance angles for the Cyt *c*−Au moves downward whereas that for the bare Au shows no change. The SPR curves at the right represent higher concentrations.

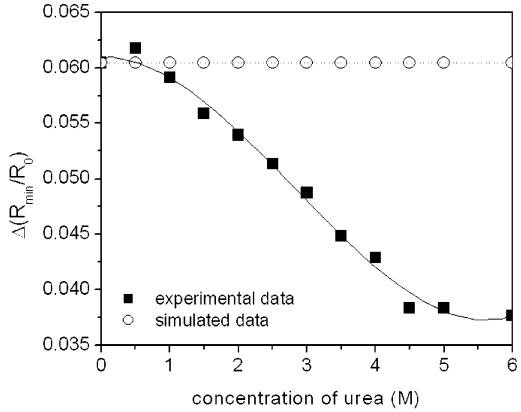

Figure 5. $\Delta(R_{min}/R_0)$ versus urea concentration from 0 to 6 M. The experimental data (squares, solid line) gradually decrease to 5 M and are saturated above 5 M, whereas the simulated data (circles, dotted line) remain unchanged, which means that $(R_{Cyt\ c}/R_0)_{min}$ is constant as a function of urea concentration. The solid line and the dotted line are polynomial fits to the experimental data and the simulated data, respectively.

because urea does not absorb at the excitation wavelength.[19] The value of ϵ' $(=n^2)$ is proportional to the concentration of urea.[26] Therefore, the refractive index of the spatial layer on a bare Au surface increases proportionally to the urea concentration, as shown in Figure 4a. When the Cyt *c* is self-assembled on the gold surface, the Cyt *c* layer in the evanescent wave region contributes to the change in the complex refractive index, and the new complex refractive index N' on Cyt *c* layer under different urea concentrations is expressed by $N' = xN_{Cytc} + (1 - x)n_{urea}$, where x is the volume fraction of the protein, $N_{Cyt\ c}$ is the complex refractive index of Cyt *c*, and n_{urea} is the refractive index of urea.[27] Then, the real and imaginary parts of the dielectric constant of Cyt *c* layer are expressed as

$$\epsilon' = [xn_{Cytc} + (1 - x)n_{urea}]^2 - {k_{Cytc}}^2 \quad (1)$$

$$\epsilon'' = 2[xn_{Cytc} + (1 - x)n_{urea}]k_{Cytc} \quad (2)$$

With these parameters, we simulated SPR curves for both bare Au and Cyt *c*−Au under the same conditions, assuming that the urea in contact with Cyt *c* does not affect the dielectric constant of Cyt *c* on Au. The reflectivity functions for bare Au and Cyt *c*−Au are expressed, respectively, as[28]

$$\frac{R_{Au}}{R_0} \approx 1 - \frac{4\Gamma_{in}\Gamma_{rad}}{(k_x - \Gamma^r)^2 + (\Gamma_{in} + \Gamma_{rad})^2} \quad (3)$$

and

$$\frac{R_{CytC}}{R_0} \approx 1 - \frac{4\Gamma_{in}\Gamma_{rad}}{(k_x - \Gamma^{r'})^2 + (\Gamma_{in} + \Gamma_{rad})^2} \quad (4)$$

where $\Gamma^r = \mathrm{Re}[k_x^0] + \mathrm{Re}[\Delta k_x^{Au}]$, $\Gamma^{r'} = \mathrm{Re}[k_x^0] + \mathrm{Re}[\Delta k_x^{Au}] + \Delta k_x^{Cytc}$, $\Gamma_{in} = \mathrm{Im}[k_x^0]$, $\Gamma_{rad} = \mathrm{Im}[\Delta k_x^{Au}]$, and $k_x = k_x^0 + \Delta k_x^{Au} + \Delta k_x^{Cytc}$, where we have labeled the real and imaginary quantities with Re and Im, respectively. The k_x^0 is the surface plasmon polariton wavenumber at the interface of two semi-infinite media, and Δk_x^{Au}, Δk_x^{Cytc} are perturbations to the wavenumber k_x^0 in the presence of the additional phases and interfaces. Analytical expressions for these quantities have been presented elsewhere.[29−31] Two sets of SPR curves depending on urea concentration were calculated using known optical properties[25] and from eqs 3 and 4. The results show that both SPR curves shift proportionally to the increase in urea concentration, as in Figure 4a, but show no change in minimum reflectivity at each SPR angle. The minimum reflectivity $(R_{Au}/R_0)_{min}$ at each SPR angle for bare Au was subtracted from the minimum reflectivity $(R_{Cytc}/R_0)_{min}$ for Cyt *c*−Au to form the difference, providing a plot of $\Delta(R_{min}/R_0)$ versus urea concentration (simulated data in Figure 5). These values are compared with the corresponding sets of data derived from Figure 4. The experimental data gradually decreased in $\Delta(R_{min}/R_0)$ as a function of urea concentration, while the $\Delta(R_{min}/R_0)$ from the

(26) Kurihara, K.; Suzuki, K. *Anal. Chem.* **2002**, *74*, 696−701.
(27) Shank-Retzlaff, M. L.; Sligar, S. G. *Anal. Chem.* **2002**, *72*, 4212−4220.
(28) Chah, S.; Hutter, E.; Roy, D.; Fendler, J. H.; Yi, J. *Chem. Phys.* **2001**, *272*, 127−136.
(29) Hutter, E.; Fendler, J. H.; Roy, D. *J. Appl. Phys.* **2001**, 90, 1977−1985.
(30) de Bruijin, H. E.; Altenburg, B. S. F.; Kooyman, R. P. H.; Greve, J. *Opt. Commun.* **1991**, *82*, 425−432.
(31) Hutter, E.; Fendler, J. H.; Roy, D. *J. Phys. Chem. B* **2001**, *105*, 11159−11168.

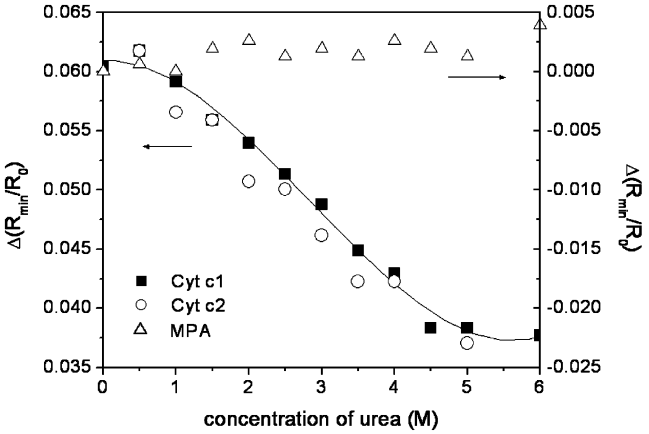

Figure 6. Urea-driven denaturation and renaturation of the Cyt *c*−Au film. The circles were plotted by repeating the experiment after the Cyt *c* on Au was denatured by urea (solid squares from 0 to 6 M urea). The $\Delta(R_{min}/R_0)$ shows the same behavior in both experiments, which implies that the denaturation of Cyt *c* on Au is reversible. The solid line is a third-order polynomial fit to experimental data. The data from the SAM prepared from MPA were plotted to compare the differences in $\Delta(R_{min}/R_0)$. The left scale is for Cyt *c*, and the right scale is for MPA.

simulated results showed no change. The commonly seen shifts to the right are caused by the urea solutions. The downward shift in reflectivity observed in our experiments, however, cannot be explained by the refractive index change of the solution itself. Changes in optical properties or changes in thickness of the layer should be considered in making an interpretation of the phenomenon. Therefore, it is concluded that the assumption that the urea in contact with Cyt *c* does not affect the dielectric constant of Cyt c on Au is false. The structure of the Cyt *c* on Au is affected by urea-driven denaturation ($N \overset{urea}{\leftrightarrow} D$), resulting in changes arising from protein unfolding. Here, it is noted that the effect of a denaturant on the conformational changes of Cyt *c* can be monitored by comparing the SPR signal obtained in the presence of a denaturant to the SPR signal in the absence of a denaturant.

Renaturation of Cyt *c* on Gold Surface. Most proteins seldom recover their activity once they are denatured, especially at a solid surface, but the ability to renature is an important factor when they are considered as catalysts or sensors. Interestingly, the Cyt *c* in solution phase undergoes reversible denaturation. To investigate the reversibility of Cyt *c* denaturation on a solid surface, we repeated denaturation and renaturation. Figure 6 shows the effect of urea-driven denaturation and renaturation on Cyt *c*. We repeated a second cycle after finishing the denaturation of Cyt *c* with urea from 0 to 6 M. Two sets of experiments were performed on the same Cyt *c* system (squares and circles in Figure 6). As can be seen, the results agree closely with each other, showing that the denaturation of Cyt *c* is reversible. In addition, this result also shows that this method is reproducible under the same conditions.

As a control, we also present data for the Au surface modified with MPA, which is not denatured by urea. The SPR curves obtained from the MPA−Au shifted to the right as a function of urea concentration (not shown here) but showed no downward shift in the minimum reflectivity at the SPR angle (triangles, Figure 6) as expected. These observations further validate the interpretation of Cyt *c* data obtained in the presence of urea.

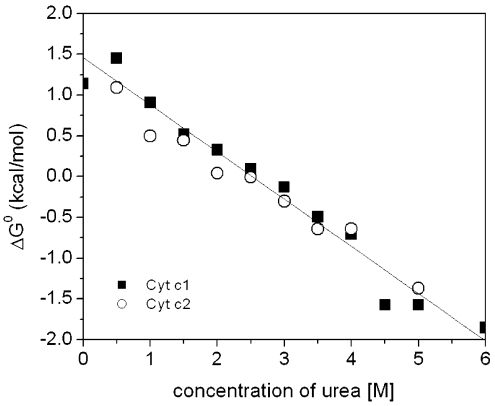

Figure 7. Gibbs free energy change $\Delta G°$ versus urea concentration, derived from the experimental data in Figure 6. The $\Delta G°_{water}$ for denaturation of Cyt *c* was calculated to be 1.5 kcal/mol.

Gibbs Free Energy Change $\Delta G°$ for the Denaturation of Cyt *c* at the Solid−Liquid Interface. From data presented in Figure 6, we were able to calculate the Gibbs free energy change for the denaturation of Cyt *c* (Figure 7). The reflectivity data in Figure 6 were fitted using the equation

$$\Delta\frac{R_{min}}{R_0} = (f_N)\left(\Delta\frac{R_{min}}{R_0}\right)_N + (f_D)\left(\Delta\frac{R_{min}}{R_0}\right)_D \quad (5)$$

where $\Delta(R_{min}/R_0)_X$ is the reflectivity change and f_X is the fraction of Cyt *c* in the state X where X = N represents the native state and X = D represents the denatured state. The values for these variables were determined from the data at each concentration of denaturant. These values were then substituted into the equation

$$K_{eq} = \frac{[D]_{eq}}{[N]_{eq}} = \frac{f_D}{f_N} = \frac{f_D}{1 - f_D} \quad (6)$$

from which the free energy change for denaturation $\Delta G°$ was found using

$$\Delta G° = -RT \ln K_{eq} \quad (7)$$

and the Gibbs free energy change for denaturation in water $\Delta G°_{water}$ could be extrapolated from a linear fit

$$\Delta G°_{water} = \Delta G° - 0.579[\text{urea}] \quad (8)$$

to the data obtained from eq 7.

The $\Delta G°_{water}$ for denaturation of Cyt *c* bound to the gold surface was calculated to be 1.5 kcal/mol. This value is ∼4 times less than the published value for the free energy of denaturation of Cyt *c* in solution (∼6.4 kcal/mol).[23] This difference could indirectly explain the decrease in bioactivity when Cyt *c* is attached to Au.

If the Gibbs free energy change of denaturation depends on experimental conditions such as the thickness of the Au layer or the wavelength of incident light, it would be problematic. To examine the reproducibility and reliability of the SPR method in the estimation of $\Delta G°$ for the denaturation of biomolecules on a

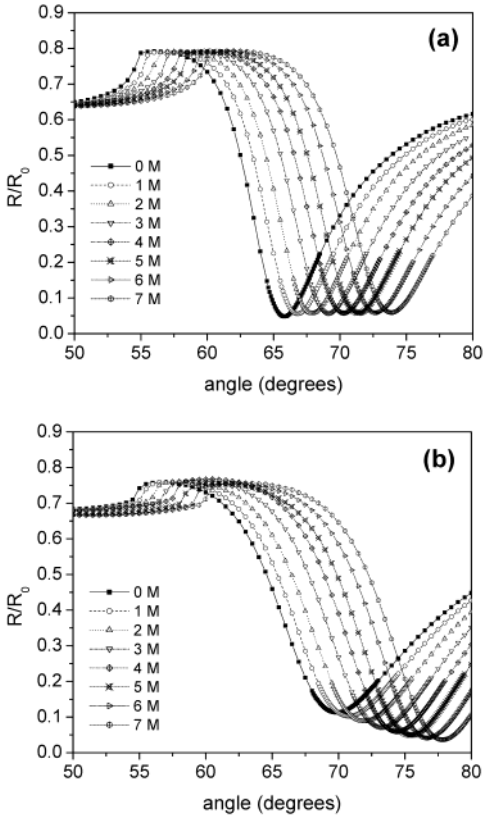

Figure 8. Angle-resolved SPR curves as a function of urea concentration (a) for 50-nm bare Au followed by 1-nm Cr layer and (b) for Cyt *c*−Au. In comparison with Figure 4, the absolute value in reflectivity at each SPR angle is seen to be different. Nonetheless, it shows the same trends in that the reflectivity at resonance angles for the Cyt *c*−Au moved downward whereas that for the bare Au maintained the same height. The SPR curves at right represent higher urea concentrations.

solid, the measurements of urea-driven SPR curves were repeated under two different conditions. One condition was the 50-nm Au film on 1-nm Cr (Au/Cr) by excitation at 632.8 nm, and the other was the 50-nm Au film by excitation at 840 nm in the near-IR.

For the preparation of 50-nm Au surface, we evaporated Au followed by a Cr layer on SF10 glass with the same procedure that was used for an Au/Ti layer. The thicknesses of Au and Cr layers were monitored using QCM. Again, we measured angle-resolved SPR curves at increasing urea concentrations. Sequentially, the Au film was covered with Cyt *c* until the binding was saturated, and another set of SPR curves were obtained at increasing urea concentration. Figure 8 displays two sets of SPR curves obtained from the Au/Cr film at 632.8 nm. The initial SPR curves (measured at 0 M urea) for bare Au and Cyt *c*−Au in Figure 8 are different from those in Figure 4 in terms of θ_{SPR}, width, and $(R/R_0)_{min}$ because they have different layers and use different incident wavelengths. Nevertheless, they show a similar trend in which $(R_{Cyt\,c}/R_0)_{min}$ decreases at higher urea concentration up to 6 M, whereas $(R_{Au}/R_0)_{min}$ is unchanged. The different behaviors shown in Figure 8 are more obvious than in Figure 4. The sensitivity of SPR is dependent upon the thickness of the

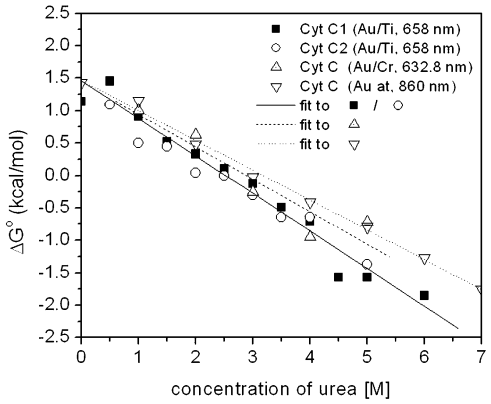

Figure 9. Gibbs free energy change $\Delta G°$ versus urea concentration, calculated from three different experimental conditions: (1) 44-nm Au on 2-nm Ti at 658 nm; (2) 50-nm Au on 1-nm Cr at 632.8 nm; and (3) 50-nm Au at 840 nm. The $\Delta G°_{water}$ for denaturation of Cyt *c* is 1.5 kcal/mol in each of these three conditions, even though the data show some spread at higher concentrations of urea.

metal layers. A calculation using the Fresnel equation indicates that ~50 nm is the optimum Au thickness for high sensitivity. It is noted that this condition also holds for changes in $(R_{Cyt\,c}/R_0)_{min}$ at different urea concentrations. The data from the second set of conditions, 50-nm Au at 840 nm, were obtained using a commercialized SPR sensor (Spreeta, Texas Instruments), which has been described elsewhere in detail.[24]

Data for Au/Cr at 632.8 nm (Figure 8) and Au at 840 nm (not shown here) were plotted using eqs 5−7 to give $\Delta G°$ versus urea concentration (Figure 9). The Cyt *c* data in Figure 7 were also displayed for comparison. The data show more dispersion at higher urea concentrations. This spread may come from the differences in uniformity in the film, coverage of Cyt *c* on Au, or the temperature of each experimental condition. Nonetheless, three linear fits to each experimental set closely match one another. Of special note is that the Gibbs free energy change for denaturation in water has the same value, 1.5 kcal/mol, for each determination.

It is known that the free energy for the denaturation of Cyt *c* bound to a surface is less than in the free state,[32,33] but to our knowledge, the measurement reported here is the first time a quantitative value has been determined. This method can be extended to the calculation of the Gibbs free energy change for the denaturation of other biomolecules at solid surfaces because the technique to build the corresponding layers of biomolecules including the ones with no thiol functional groups is already established.[34] Consequently, we expect that this work will serve as an example of how SPR measurements can contribute to our understanding of fundamental properties of biomolecules at solid−liquid interfaces.

ACKNOWLEDGMENT

S.C. was supported by the Postdoctoral Fellowship Program of Korea Science & Engineering Foundation (KOSEF). C.V.K. acknowledges support by NSF DMR-0300631. This work was also supported by the National Science Foundation under NSF MPS-0313996.

Received for review December 1, 2003. Accepted January 28, 2004.

AC035416K

(32) Kumar, C. V.; McLendon, G. L. *Chem. Mater.* **1997**, *9*, 863−870.
(33) Ball, A.; Jones, R. A. L. *Langmuir* **1995**, *11*, 3542−3548.
(34) Zimmermann, H.; Lindgren, A.; Schuhmann, W.; Gorton, L. *Chem. Eur. J.* **2000**, *6*, 592−599.